A FRACTURE CRITERION FOR NOTCHED SAMPLES OF HIGH-STRENGTH PEARLITIC STEEL

J. TORIBIO
Department of Engineering, University of La Coruña
E.T.S.I. Caminos, Pol. Sabón, P.12-14, 15141 Arteixo, La Coruña, Spain

ABSTRACT

In this paper a fracture criterion is proposed for high-strength pearlitic steel subjected to multiaxial stress states produced by notches of very different geometries. The research includes a fractographic study of the microscopic modes of fracture by scanning electron microscopy, and a numerical analysis by means of an elastic-plastic finite element method, to compute the stress state in the samples at the fracture instant. The results demonstrate that fracture takes place when the distortional part of the strain energy density reaches a critical value over a critical distance characteristic of the microstructure of the material.

KEYWORDS

High-strength steel, pearlitic steel, notched samples, triaxial stress state, fractographic analysis, microscopic fracture modes, fracture criterion.

INTRODUCTION

Although many effort has been made in the past to study fracture processes in cracked components, relatively few work has been devoted to the analysis and understanding of the mechanisms of failure phenomena in notched specimens. However, defects like notches (i.e., with given root radius) are very frequent in structural components (Elices, 1985), due to the particular working conditions (e.g. in anchorages for prestressed concrete). In addition, notched specimens generate a triaxial stress distribution near the notch (cf. cracked ones), which allows a detailed analysis of the macroscopic and microscopic fracture mechanisms (Mackenzie *et al.*, 1977). Because of the possibility of generating variable stress states in the vicinity of the notch, notched specimens have been recommended for studying hydrogen embrittlement phenomena (Thompson, 1985), because hydrogen diffuses towards the point of maximum hydrostatic stress, which depends on the notch geometry.

The final aim of this paper is the establishment of a fracture criterion for notched samples of high-strength pearlitic steel, which provides insight on the factors influencing the fracture of that steel under triaxial stress states produced by notches and the relationship between the macroscopic variables and the microscopic parameters which affect the fracture process itself.

EXPERIMENTAL PROGRAMME

The material was a hot rolled pearlitic steel whose stress-strain curve can be modelled according to the following Ramberg-Osgood equation:

$$\varepsilon = \sigma/199000 + (\sigma/2100)^{4.9}, \quad \sigma \text{ in MPa} \tag{1}$$

Four axisymmetric notched geometries of maximum and minimum notch depths and radii were chosen, as shown in Fig.1, with the following dimensions:

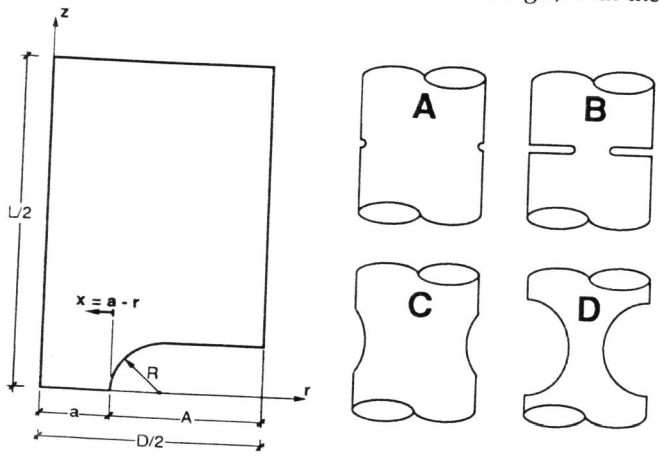

Sample	R/D	A/D
A	0.03	0.10
B	0.05	0.39
C	0.36	0.10
D	0.40	0.39

Fig. 1. Notched geometries.

Two fracture tests were performed for each geometry, recording continuously the load and the relative displacement between two points. Geometries A and C present a macroscopically brittle behaviour prior to fracture; geometry B shows a negligible decrease in load; geometry D is the only one that presents a macroscopically ductile behaviour prior to fracture, with a clear decrease in load. These macroscopically brittle or ductile behaviours are defined on the basis of the load-displacement curve for the fracture tests (brittle if the curve has positive slope; ductile when the curve presents negative slope). In any case, however, there is a correspondence between macroscopic behaviour and microscopic topography, as it can be seen after fractographic analysis. Fracture is assumed to occur at the maximum load point for all geometries.

FRACTOGRAPHIC ANALYSIS

Three conventional microscopic fracture modes were observed: Micro-Void Coalescence (MVC, zone in which the fracture process initiates), Cleavage-like (C, zone corresponding to unstable fracture) and Shear Lip (L, zone of final fracture when it is clearly ductile). The summary of the microscopical analyses for all geometries is the following:

- Geometry A presents a fracture surface macroscopically plane, with a microscopic appearance consisting of oriented cleavage. The directions of orientation start from a point which represents, therefore, the point in which the fracture process initiates. At this point, and at the opposite one, microscopic zones created by micro-void coalescence are observed. (see Fig. 2)
- Geometry B shows a fracture surface macroscopically plane, with a microscopic fracture feature created by cleavage without a preferential orientation. The external ring, of around 75 mm depth, has a topography formed by micro-void coalescence plus cleavage. In this area the failure process initiates.
- The fracture surface of geometry C is plane from the macroscopic point of view. The microscopic feature is of cleavage-like type, with a predominant orientation starting from the initiation point, similar to geometry A.
- Geometry D shows a typical *cup and cone* fracture surface (macroscopically). Microscopically, fracture initiates at the center of the sample, by micro-void coalescence, the external ring consisting of shear lips.

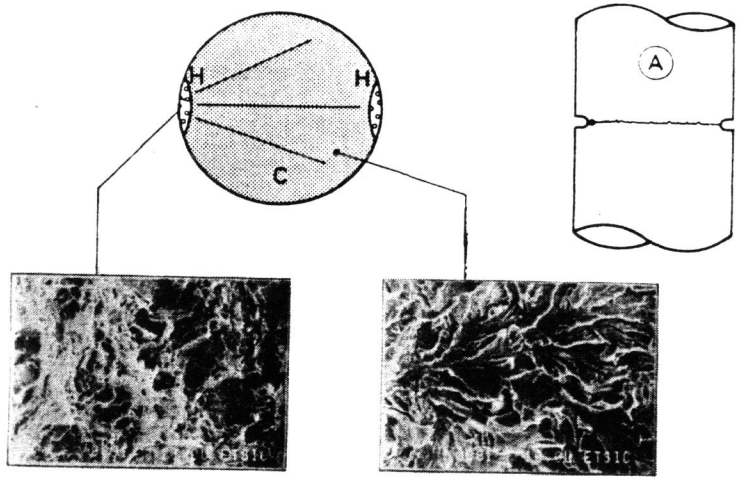

Fig. 2. Fractographic analysis of geometry A
(H: Micro-Void Coalescence, C: Cleavage).

NUMERICAL COMPUTATIONS

In a fracture test the macroscopic external variables (force, displacement,....) are measured. To find the distribution of macroscopic internal variables (stress, strain, strain energy density,...) at any time, and particularly at the moment of fracture, the Finite Element method with an elastic-plastic code was applied, using a Von Mises yield surface with incompressible constitutive equation (Classical Plasticity). The relationship between equivalent stress and strain is introduced by means of a Ramberg-Osgood equation (1).

The external load was introduced step by step, by applying nodal displacements. An improved Newton-Raphson Method was adopted, which modified the tangent stiffness matrix at each step. The finite elements used in the computations were isoparametric with second-order interpolation (eight -node quadrilaterals and six-node triangles).

In Fig. 3 the FEM computations for geometry C are compared with the experimental results, plotting load vs. displacement during the test. As shown in the Figure, the agreement is very good, since the numerical results are always within the experimental scatter band (two fracture tests for each geometry).

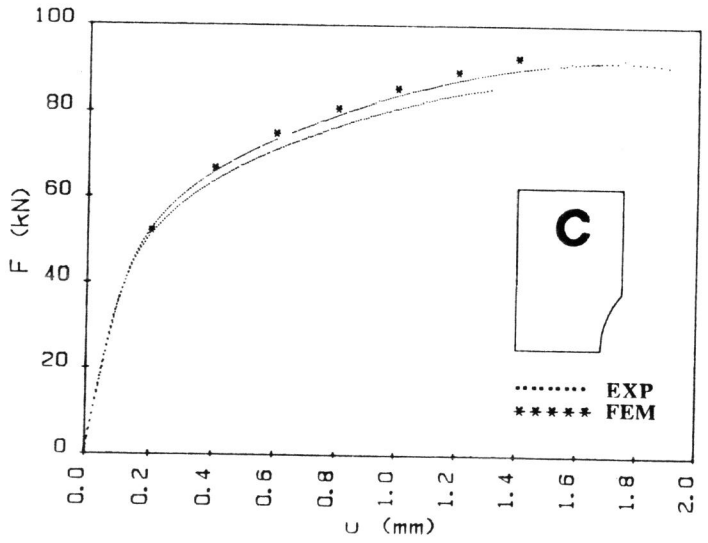

Fig. 3. Comparison between numerical (FEM) and experimental results.

FORMULATION OF A FRACTURE CRITERION

The formulation of the fracture criterion is based on the two following conditions:

- The variable governing the fracture process should have an energetic meaning (e.g. strain energy density).
- The fracture criterion should not be punctual, but applied over a critical region dependent on the microstructure of the material.

Two variables with energetic meaning will be considered, and their distribution at the fracture instant analyzed on the basis of the finite element results:

(i) The *strain energy density*, defined as follows:

$$\omega = \int_{0}^{\varepsilon} \sigma \bullet d\varepsilon \qquad (2)$$

where σ and ε are the stress and strain tensors, respectively. It has been used by Guillemot (1976) and Sih (1985) as the critical variable for fracture processes (*strain energy density criterion*).

(ii) The *effective or equivalent stress* in the Von Mises sense, whose expression is:

$$\bar{\sigma} = (3\, \sigma' \bullet \sigma' / 2)^{1/2} \qquad (3)$$

where σ' is the stress deviatoric tensor. This variable is a direct function of the distortional part of the strain energy density (related to shape changes, in opposition to the dilatational part, related to volume changes).

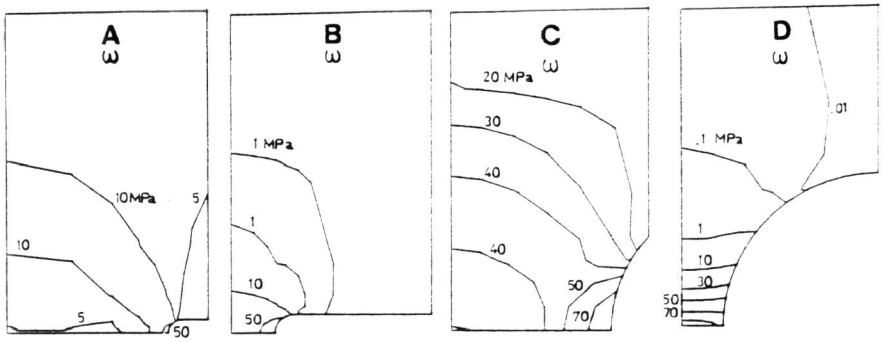

Fig. 4. Distribution of strain energy density (ω) at the fracture instant.

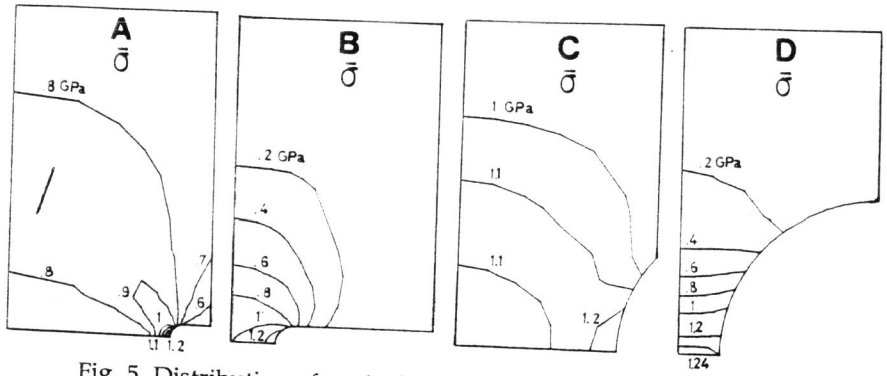

Fig. 5. Distribution of equivalent stresss ($\bar{\sigma}$) at the fracture instant.

Figs. 4 and 5 show the distribution of strain energy density and equivalent stress, respectively, at the fracture instant. The plastic zone (line of equivalent stress equal to the yield strength, 0.6 GPa) clearly exceeds the fracture zone, and seems to have no influence on the fracture process, produced by cleavage. On the other hand, the strain energy density and the equivalent stress could be the governing variables, which requires a more detailed analysis to elucidate which is the relevant one. Both are consistent with the fractographic analysis, since the fracture is peripherical (maximum at the notch tip) in geometries A, B and C, and central (maximum at the center of the section) in geometry D.

To establish the criterion, it is necessary to know the average values of the governing variables over the fracture zone or critical region Such averages were numerically calculated from the results of the finite element analysis, i.e.:

$$< \xi > = \frac{1}{\pi(a^2-r_c^2)} \int_0^{2\pi} \int_{r_c}^{a} \xi(r)\, r\, dr\, d\theta \qquad (4)$$

where $< >$ represents space average, a is the radius of the net section (see Fig. 1), r_c the radial coordinate which defines the end of the critical zone ($r_c = a - x_c$), and ξ a variable representing the strain energy density or the equivalent stress.

Given the small size of the critical area, one simple method to compute the average value (4) with a relative error less than 1%, consists of substituting the average value by the value at the medium point, as follows:

$$< \xi > = \xi (a - x_c/2) \qquad (5)$$

The depth of the critical region (x_c) will be several times –but never less than–the size of the cleavage facet (75 μm for the steel under analysis), which coincides with the prior austenite grain size and represents the minimum microstructural fracture unit in pearlitic steels (Park and Bernstein, 1979; Lewandowski and Thompson, 1986).

Table 1 shows the average values at the fracture instant of the strain energy density and the effective or equivalent stress (directly related to the distortional part of the strain energy density). Averages are calculated over critical sizes (x_c) equal to one, two and three times the size of the cleavage facet (x_{CL}).

Table 1. Critical values of ω and $\bar{\sigma}$ (in MPa).

	$x_c = x_{CL}$		$x_c = 2\,x_{CL}$		$x_c = 3x_{CL}$	
Geometry	ω	$\bar{\sigma}$	ω	$\bar{\sigma}$	ω	$\bar{\sigma}$
A	104.9	1299	84.0	1243	63.2	1188
B	115.3	1324	103.5	1299	95.0	1281
C	96.6	1287	94.9	1283	93.2	1278
D	83.0	1251	82.8	1251	83.0	1251

The equivalent stress is seen to be the relevant variable in order to formulate the fracture criterion, but not the strain energy density. The optimum distance of applicability is two cleavage facets, although results are not substantially different for one and three cleavage facets.

A simple general criterion can thus be formulated on the basis of the distortional part of the strain energy density, or accordingly, the effective or equivalent stress in the Von Mises sense, since the latter is directly related to the former. This criterion can be formulated in the following way:

Fracture will take place when the distortional part of the strain energy density (or, accordingly, the effective or equivalent stress in the von Mises sense) reaches a critical value over a critical region characteristic of the microstructure of the material.

In mathematical form:

$$< \bar{\sigma} > = \bar{\sigma}_o \quad \text{over} \quad x_c \qquad (6)$$

where $< \bar{\sigma} >$ is the average equivalent stress at the fracture instant, $\bar{\sigma}_o$ the critical equivalent stress of the material and x_c the depth of the critical region. For the pearlitic steel used in this research, the characteristics of strength and microstructure (parameters of the material) are:

$$\bar{\sigma}_o = 1260 \pm 10 \text{ MPa}$$
$$x_c = 2\,x_{CL} = 150\ \mu\text{m}$$

which can be obtained by the procedure described in this paper: fracture tests on notched bars and numerical analysis to find the distribution of internal macroscopic variables at the fracture instant.

CONCLUSIONS

1. A relationship was found between the macroscopic and the microscopic fracture modes: When the fracture is peripheral and plane, the mechanism consists of cleavage (initiated by MVC) whereas when the fracture is central with *cup and cone* shape, the failure process is by MVC.

2. The distributions of macroscopic internal variables at the fracture instant, obtained by numerical methods, were consistent with fractographic analysis, since the maximum value of the macroscopic governing variables were achieved in the area where microscopic fracture initiated.

3. A fracture criterion was formulated for notched samples of high-strength pearlitic steel: Fracture will take place when the distortional part of the strain energy density (or, accordingly, the effective or equivalent stress in the von Mises sense) reaches a critical value over a critical region characteristic of the microstructure of the material.

Acknowledgments

This work was supported by the Spanish Office for Science and Technological Research (CICYT), under Grant MAT91-0113-CE. The author would like to thank Professor M. Elices, head of the Material Science Department of the Polytechnical University of Madrid, for his encouragement and assistance, to Dr. A.M. Lancha, CIEMAT, Spain, for the SEM fractographic analysis, and to Mr. J. Monar, *Nueva Montaña Quijano Co.*, Santander, Spain, for providing the steel used in the experimental programme. In addition, the author wishes to express his gratitude to the *Colegio de Ingenieros de Caminos, Canales y Puertos–Demarcación de Galicia*, Spain, for the financial support of technical trips during the final stages of this work.

REFERENCES

Elices, M. (1985) 'Fracture of steels for reinforcing and prestressing concrete', in *Fracture Mechanics of Concrete*, pp. 226-271 (Sih, G.C. and DiTommaso, A., Eds.). Martinus Nijhoff Publishers, Dordrecht, The Netherlands.

Guillemot, L.F. (1976) 'Criterion for crack initiation and spreading', *Engng. Fracture Mech.* **8**, 239-253.

Lewandowski, J.J. and Thompson, A.W. (1986) 'Effects of the prior austenite grain on the ductility of fully pearlitic eutectoid steel', *Metall. Trans.* **17A**, 461-472.

Mackenzie, A.C., Hancock, J.W. and Brown, D.J. (1977) 'On the influence of state of stress on ductile failure initiation in high strength steels', *Engng. Fracture Mech.* **9**, 167-188.

Park, Y.J. and Bernstein, I.M. (1979) 'The process of crack initiation and effective grain size for cleavage fracture in pearlitic eutectoid steel', *Metall. Trans.* **10A**, 1653-1664.

Sih, G.C. (1985) 'Mechanics and physics of energy density theory', *Theor. Appl. Fracture Mech.* **4**, 157-173.

Thompson, A.W. (1985) 'Hydrogen assisted fracture at notches', *Mater. Sci. Tech.* **1**, 711- 718.